RESULTS ON THE CEV PROCESS, PAST AND PRESENT

D. R. Brecher and A. E. Lindsay

March 10, 2010

We consider the Constant Elasticity of Variance (CEV) process, carefully revisiting the relationships between its transition density and that of the non-central chi-squared distribution, and establish a symmetry principle which readily explains many classical results. The principle also sheds light on the cases in which the CEV parameter exceeds one and the forward price process is a strictly local martingale. An analysis of this parameter regime shows that the widely-quoted formula for the price of a plain vanilla European call option requires a correction term to achieve an arbitrage free price. We discuss Monte Carlo simulation of the CEV process, the specifics of which depend on the parameter regime, and compare the results against the analytic expressions for plain vanilla European option prices. We find good agreement. Using these techniques, we also verify that the expected forward price is a strictly local martingale when the CEV parameter is greater than one.

Keywords: CEV process, Bessel process, local martingale.

1. INTRODUCTION

Pricing derivatives under the assumption of constant volatility, as in the classic Black-Scholes-Merton model [5, 25] of option pricing, is well-known to give results which cannot be reconciled with market observations, although these problems did not widely manifest themselves until the 1987 market crash. After this event, the so-called *volatility smile* or *volatility skew* became common place in equity markets.

The volatility smile is a market phenomenon whereby the Black-Scholes implied volatility of an option exhibits a dependence on the strike price. There has been an ongoing interest in capturing and predicting the properties of the volatility smile and consequently a variety of models have been proposed and studied (*e.g.* local volatility models [9, 11] and stochastic volatility models [18, 19, 21]). The constant elasticity of variance (CEV) process was first proposed by Cox &

d.brecher@fincad.com
FINCAD
Suite 1750, Central City
13450 102nd Avenue
Surrey
B.C. V3T 5X3
Canada
ael@math.ubc.ca
Mathematics Department
University of British Columbia
Vancouver
B.C. V6T 1Z2
Canada

[1]Support is gratefully acknowledged from the MITACS Accelerate program.

Ross [8] as an alternative to the Black-Scholes model of stock price movements and, indeed, the model does give rise to a volatility skew.

The CEV model is a continuous time diffusion process satisfying

$$\mathrm{d}F = \sigma F^{\alpha}\,\mathrm{d}W, \qquad F(0) = F_0, \tag{1}$$

where $F(t)$ is the state variable representing the forward price of some underlying asset at time t and W is a standard Brownian motion. The parameter α is called the elasticity and we take $\alpha \neq 1$ to distinguish (1) from the Black-Scholes model. The omission of a drift term in (1) is made purely for convenience as it has no qualitative effect on the dynamics of the process, but simplifies the resulting algebra considerably.

Note that σ in (1) has dimensions of $F^{1-\alpha}/\sqrt{T}$, and we account for this by taking

$$\sigma = \sigma_{\mathrm{LN}} F_0^{1-\alpha},$$

where σ_{LN} is an effective "lognormal volatility" with the standard dimension of $1/\sqrt{T}$. By considering at-the-money options, the origin of the volatility skew in the CEV model can be understood heuristically from this expression: models with $\alpha < 1$ ($\alpha > 1$) give rise to skews of negative (positive) slope. Since the equity markets usually exhibit volatility skews of negative slope, the CEV process with $\alpha > 1$ is rarely considered in the literature.

Feller's work [15] on singular diffusion processes underpins much of our theoretical understanding of (1) and demonstrates that the CEV process admits three distinct types of solutions according to the parameter regimes $\alpha < 1/2$, $1/2 \leq \alpha < 1$ and $\alpha > 1$. Cox & Ross [8, 6] used an explicit formula for the transition density in the case $\alpha < 1$ to establish closed-form prices for European options in terms of a sum of incomplete gamma functions. Schroder [27] established a connection between this pricing formula and the non-central chi-squared distribution.

Emanuel & MacBeth [14] approached the case $\alpha > 1$ by constructing the relevant norm-preserving density function. In this parameter regime, it was observed by integrating this density that $\mathbb{E}[\, F_T |\, F_0] \neq F_0$. Lewis [23] shows that this is attributable to the fact that F_T is a strictly local martingale when $\alpha > 1$ and then demonstrates that this behavior must be accounted for in order to achieve an arbitrage free option pricing formula. We will argue that due to the local martingale property of the process for $\alpha > 1$, the widely-quoted call price in this case (see, *e.g.*, [20]; the origin of these results seems to be [27]) does not represent an arbitrage free value unless augmented with a correction term, which we derive to obtain a slightly different expression. This has been noticed by Lewis [23], and discussed by Atlan & Leblanc [4]. We provide a different perspective here, and verify the result via Monte Carlo simulation.

This work aims to provide a clear overview of classical results regarding the CEV process and to fill some of the gaps present in the aforementioned literature.

The relationship between the CEV process, the squared Bessel process and the non-central chi-squared distribution is also clarified. Closed-form option pricing formulae are developed in light of these results, and Monte Carlo simulation of (1) is used as a means of verification. A useful tool in our analysis is a symmetry relationship between solutions of the CEV process for $\alpha < 1$ and $\alpha > 1$. The paper is structured as follows.

In §2, we make some general remarks about the CEV process. In §3, the results of Feller are revisited including his boundary point classification theorems. The relationship between the CEV process (1) and the CIR [7] and Heston [19] models is also discussed. In §4 we examine the properties of the transition density function, highlighting the connections or otherwise with the non-central chi-squared distribution, and establish a symmetry relationship between the regimes $\alpha < 1$ and $\alpha > 1$. In §5 and §6, we compute the expected value and variance of the square root process related to (1), in addition to the expected value of F_T itself, and analyze the case $\alpha > 1$. We comment on the local martingale nature of the process in this case. In §7, we derive closed-form expressions for the prices of plain vanilla European options, directly from the transition density function, and comment on how and why that for the $\alpha > 1$ call price is different to the standard results. In §8, we discuss techniques for Monte Carlo simulation of the CEV process (1), and test them against our analytic results for both the forward price of the underlying, and the prices of plain vanilla European options. We find very good agreement. Finally in §9 we discuss our results.

2. GENERAL PROPERTIES OF THE CEV PROCESS

The CEV process applied to the forward price $F(t)$ of some underlying asset satisfies the stochastic differential equation (SDE) (1). For general values of α, there are obvious difficulties with this SDE as F goes through the origin $F = 0$ to negative values, so we take the view that (1) applies only up to the stopping time

$$\tau \equiv \inf_{t>0} \{F(t) = 0\}. \tag{2}$$

The treatment of the process after the stopping time requires consideration of the underlying financial problem. For example, when F represents some equity asset price, the stopping time (2) would indicate the time of bankruptcy. In other financial scenarios, however, F could represent an interest rate or the variance of an equity asset price, in which case a return to $F > 0$ after the stopping time would be more sensible. In this section, we establish conditions under which the origin is accessible, and discuss how the process might evolve after the stopping time (2).

It is advantageous to work with the transformed variable

$$X = \frac{F^{2(1-\alpha)}}{\sigma^2(1-\alpha)^2}. \tag{3}$$

Applying Itö's Lemma to (3) shows that X can be written as a square root process

$$\mathrm{d}X = \delta\,\mathrm{d}t + 2\sqrt{X}\,\mathrm{d}W, \tag{4}$$

where

$$\delta \equiv \frac{1-2\alpha}{1-\alpha}.$$

Equation (4) is a squared Bessel process BESQ^{δ}, with δ degrees of freedom. It is well known that for $0 \leq \delta < 2$ the origin is accessible from $X > 0$ in finite time (see, *e.g.*, [26] for a general study of Bessel processes). Given the obvious problems for negative values of X, we therefore again take the view that a path of (4) is defined only up to the stopping time

$$\tau \equiv \inf_{t>0} \left\{X(t) = 0\right\}.$$

In the next subsections, the connection between the integer δ case and diffusion in multiple dimensions is mentioned, followed by the relationship between (4) and some common stochastic volatility models.

2.1. *Integer δ*

For δ a positive integer, equation (4) is that governing the squared distance, X, from the origin of a Brownian particle in δ spatial dimensions. For a particle originating at position $(Y_1(0), \ldots, Y_\delta(0)) \in \mathbb{R}^{\delta}_{+}$ obeying $\mathrm{d}Y_i = \mathrm{d}W_i$ for $i = 1, \ldots, \delta$ where $(W_1, \ldots, W_\delta)$ are independent Brownian motions, we have that

$$X(t) = \sum_{i=1}^{\delta} \left(W_i + Y_i(0)\right)^2, \tag{5}$$

The form of (5) indicates that X is a non-central chi-squared variable with degrees of freedom δ and non-centrality parameter $\lambda = \sum_{i=1}^{\delta} Y_i^2(0)$. Accordingly, it has distribution

$$p_{X'^2}(x; \delta, \lambda) = \frac{1}{2}\left(\frac{x}{\lambda}\right)^{\nu/2} \exp\left[-\frac{x+\lambda}{2}\right] I_\nu(\sqrt{x\lambda}), \tag{6a}$$

where

$$\nu = \frac{\delta}{2} - 1 = -\frac{1}{2\,(1-\alpha)}, \tag{6b}$$

is the *index* of the squared Bessel process, and $I_\nu(x)$ is the modified Bessel function of the first kind.

Of course, δ is generally not an integer and not necessarily positive, in which case the analogy between X and Brownian particles in multiple dimensions does not apply. For $\delta \in \mathbb{R}^{+}$, however, the properties of (4) are well developed, although the case $\delta < 0$ has received less attention (see [28, 29, 17, 12, 13] and references therein).

2.2. *Connection with common stochastic volatility models*

Equation (4) is related to the CIR [7] and Heston [19] models, the former being a model of the short rate, the latter being a two-factor stochastic volatility model. In both cases, the relevant SDE is

$$\mathrm{d}X = \kappa\,(X_\infty - X)\,\mathrm{d}t + \omega\sqrt{X}\,\mathrm{d}W,$$

where X denotes the short rate in the CIR model, and the variance of some equity asset in the Heston model. The parameters κ, X_∞ and ω are generally taken to be positive, in which case X exhibits mean reversion to some long-term value X_∞, at a speed κ. Scaling X by $\omega^2/4$ gives

$$\mathrm{d}X = \kappa\left(\frac{4X_\infty}{\omega^2} - X\right)\mathrm{d}t + 2\sqrt{X}\,\mathrm{d}W, \tag{7}$$

and by comparing with (4) we see that the CEV model is thus a subset of this more general process, albeit a somewhat odd limit, in which

$$\kappa \to 0, \qquad \frac{4X_\infty}{\omega^2} \to \infty,$$

but such that the product

$$\frac{4\kappa X_\infty}{\omega^2} = \delta,$$

is held fixed. Since the model parameters are generally taken to be positive, the case for which $\delta < 0$ is rarely, if ever, discussed in this context (although see Andersen [1] in the context of credit derivatives).

3. THE FELLER CLASSIFICATION

To build a theory for the CEV process for all $\alpha \neq 1$, a general description of (4) for $\delta \in \mathbb{R}$ is required. To accomplish this, the classic analysis of Feller [15] is employed. Feller studied studied singular diffusion problems of type

$$\mathrm{d}X = (c + bX)\mathrm{d}t + \sqrt{2aX}\,\mathrm{d}W,$$

where a, b, c are constants, with $a > 0$. The associated forward Kolmogorov, or Fokker-Planck, equation, is

$$\frac{\partial p}{\partial t} = \frac{\partial^2}{\partial X^2}(aXp) - \frac{\partial}{\partial X}\left((bX + c)\,p\right), \qquad 0 < X < \infty, \qquad 0 \le t \le T, \tag{8a}$$

furnished with the initial condition

$$p(X, 0) = \delta\,(X - X_0)\,. \tag{8b}$$

CEV exponent	Dimension	Index
$-\infty < \alpha < 0.5$	$0 < \delta < 2$	$-1 < \nu < 0$
$0.5 \le \alpha < 1$	$-\infty < \delta \le 0$	$-\infty < \nu \le -1$
$1 < \alpha < \infty$	$2 < \delta < \infty$	$0 < \nu < \infty$

TABLE I
THE THREE PARAMETER REGIMES

where $\delta(x)$ is the Dirac delta function. The quantity

$$p_\delta(X_T, T; X_0)\,\Delta \equiv p(X_T, T)\,\Delta,$$

represents the approximate probability that $X(T) \in (X_T, X_T + \Delta)$, conditional on $X(0) = X_0$. To consider the process (4) in this notation, we take $b = 0$, $a = 2$ and $c = \delta$.

From a direct solution via Laplace transforms, Feller showed that (8) has very different properties according to whether

- $\delta \le 0$ or equivalently $\alpha \in [0.5, 1)$: the boundary $X = 0$ is attainable and absorbing.
- $0 < \delta < 2$ or equivalently $\alpha < 0.5$: the boundary $X = 0$ is attainable, and can be absorbing or reflecting.
- $\delta > 2$ or equivalently $\alpha > 1$: the boundary $X = 0$ is not attainable.

These three parameter regimes are summarized in Table I.

It follows directly from (8a) that

$$\frac{\partial}{\partial t}\int_0^\infty p_\delta(X, T; X_0)\,\mathrm{d}X = f(t) \equiv -\lim_{X\to 0}\left[\frac{\partial}{\partial X}\left(aXp_\delta\right) - (bX + c)\,p_\delta\right], \tag{9}$$

where $f(t)$ is the probability flux at the origin $X = 0$ which, depending on the value of δ, is not necessarily zero. The boundary $X = 0$ may be accessible and absorbing. Probability mass can thus be lost, resulting in a defective transition density which does not integrate to unity. In this case, it is said that solutions of (8) are norm-*decreasing* in the sense that

$$\int_0^\infty p_\delta(X, T; X_0)\,\mathrm{d}X < 1. \tag{10}$$

A norm-*preserving* solution, on the other hand, satisfies (10) but with an equality replacing the inequality.

4. THE TRANSITION DENSITY FUNCTION

The solutions of the Fokker-Planck equation (8) are discussed by Feller [15]. In the three following subsections, the parameter regimes of Table I are discussed.

4.1. *The case $\delta \leq 0$*

For $\delta \leq 0$, or equivalently $\alpha \in [0.5, 1)$, equation (8) can be furnished with arbitrary initial conditions to uniquely determine a norm-decreasing solution. No boundary conditions at $X = 0$ can be imposed; the boundary is naturally absorbing. Hitting the $X = 0$ boundary in (4) is equivalent to hitting the $F = 0$ boundary in the original CEV process (1), so that process is also absorbed at the origin.

The unique fundamental solution of the Fokker-Planck equation (8) in this case is

$$p_\delta(X_T, T; X_0) = \frac{1}{2T}\left(\frac{X_T}{X_0}\right)^{\nu/2} \exp\left[-\frac{X_T + X_0}{2T}\right] I_{-\nu}\left(\frac{\sqrt{X_T X_0}}{T}\right). \tag{11}$$

This is a special case of the solution arrived at by Feller, although there is a minor typo in his work[1]. Direct integration of the transition density (11) indicates that it is norm-*decreasing*:

$$\int_0^\infty p_\delta(X, T; X_0)\,\mathrm{d}X = \Gamma\left(-\nu; \frac{X_0}{2T}\right) < 1, \tag{12}$$

where $\Gamma(n; x)$ is the normalized incomplete gamma function

$$\Gamma(n; x) = \frac{1}{\Gamma(n)} \int_0^x t^{n-1} e^{-t}\,\mathrm{d}t. \tag{13}$$

Equation (12) is the probability that the process has not become trapped at $X = 0$ by time T. As shown in Figure 1, in the limit as $T \to \infty$, the integral vanishes, indicating that *every* path will be trapped at $X = 0$ for $\delta \leq 0$.

The full norm-*preserving* transition density should thus be given by the sum of the defective density (11) and a Dirac measure at zero with strength

$$2\left[1 - \Gamma\left(-\nu; \frac{X_0}{2T}\right)\right].$$

In other words

$$p_\delta^{\text{full}}(X_T, T; X_0) = 2\left[1 - \Gamma\left(-\nu; \frac{X_0}{2T}\right)\right] \delta\left(X_T\right) + p_\delta(X_T, T; X_0), \tag{14}$$

which is manifestly norm-preserving[2]. The coupling of a defective density with a Dirac mass at the origin has been used to study the non-central chi-squared distribution with zero degrees of freedom [28] and the squared Bessel process (4) with $\delta = 0$ [17]. Indeed, taking $\delta = 0$ in the above expression gives

$$p_0^{\text{full}}(X_T, T; X_0) = 2e^{-X_0/(2T)}\,\delta\left(X_T\right) + p_0(X_T, T; X_0),$$

[1] The term $4b^2$ in equation (6.2) of [15] should be 1. After that one may take the limit as $b \to 0$ to arrive at (11). This error was also noticed by Lewis [23].

[2] The factor of two preceding the first term of (14) arises from the fact that $\int_0^\infty \delta(x)\,\mathrm{d}x = 1/2$.

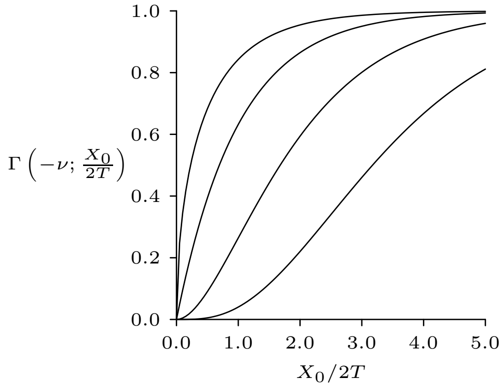

FIGURE 1.— The right hand side of (12) is plotted for several values of $\delta < 2$ (those for $0 < \delta < 2$ are relevant as per §4.2.1). At the center line, we have from left to right curves for $\delta = 1, 0, -2, -5$, or $\alpha = 0, 1/2, 3/4, 6/7$, respectively. For fixed $X_0 = (\sigma_{\mathrm{LN}}(1-\alpha))^{-2}$, all paths will eventually be trapped as each curve tends to 0 for $T \to \infty$. For fixed T, on the other hand, we see that the probability of a path having been trapped by time T increases (decreases) when X_0 decreases (increases), *i.e.* when σ_{LN} increases (decreases), or when $\alpha \to -\infty$ ($\alpha \to 1$).

which agrees with the result presented in [17]. Here, we are arguing for the extension of this to squared Bessel processes of negative dimension: for such processes, the density should be as in (14).

Finally, the transition density is related to the non-central chi-squared distribution (6) since, by inspection,

$$p_\delta(X, T; X_0) = p_{\chi'^2}\left(\frac{X_0}{T}; 4-\delta, \frac{X}{T}\right)\frac{1}{T}, \tag{15}$$

where the right-hand side is well-defined since $4 - \delta > 0$, but note that it is a function of the non-centrality parameter. Schroder, however, proves[3] that [27]

$$\int_x^\infty p_{\chi'^2}\left(X_0; 4-\delta, X\right)\,\mathrm{d}X = \chi'^2\left(X_0; 2-\delta, x\right), \tag{16}$$

where $\chi'^2(x; k, \lambda)$ is the cumulative distribution function of the non-central chi-squared distribution with degrees of freedom k and non-centrality parameter

[3]There is also a claim in [27] that $\chi'^2(x; k, \lambda) + \chi'^2(\lambda; 2-k, x) = 1$, but the proof of this relies on using the identity $I_{-n}(x) = I_n(x)$, which is true only for integer n, so in general the result will not hold.

λ. This is consistent with (12) since, substituting for $x = 0$ in (16), gives a cumulative *central* chi-squared distribution $\chi^2(x;k)$:

$$\int_0^\infty p_{\chi'^2}(X_0; 4-\delta, X)\,\mathrm{d}X = \chi^2(X_0; 2-\delta) = \Gamma\left(-\nu; \frac{X_0}{2}\right).$$

Applying (15) and (16) shows that

$$\int_0^{X_T} p_\delta(X,T;X_0)\,\mathrm{d}X = \Gamma\left(-\nu; \frac{X_0}{2T}\right) - \chi'^2\left(\frac{X_0}{T}; 2-\delta, \frac{X_T}{T}\right), \tag{17}$$

so that, including the Dirac mass in the full transition density (14), X is distributed according to

$$\Pr(X \le X_T | X_0) = \int_0^{X_T} p_\delta^{\mathrm{full}}(X,T;X_0)\,\mathrm{d}X = 1 - \chi'^2\left(\frac{X_0}{T}; 2-\delta, \frac{X_T}{T}\right). \tag{18}$$

The cumulative non-central chi-squared distribution is easily computed numerically along the lines of [10]. This method uses the fact that

$$\chi'^2(x;k,\lambda) = \sum_{i=1}^\infty \frac{e^{-\lambda/2}(\lambda/2)^i}{i!}\chi^2(x;k+2i).$$

To avoid numerical difficulties, the sum should be performed starting from the $i = \lfloor \lambda/2 \rfloor$ term for which the coefficient of $\chi^2(x;k+2i)$ is a maximum, and should then proceed for increasing and decreasing i until convergence is reached in both directions.

4.2. *The case* $0 < \delta < 2$

For $0 < \delta < 2$, or equivalently $\alpha < 0.5$, the boundary $X = 0$ is accessible, just as when $\delta \le 0$. However, the positive drift in (4) means that a path hitting $X = 0$ will be pushed back into the region $X > 0$ if the process is continued past the stopping time. When such a path hits $X = 0$, we may either impose an absorbing boundary and end the process, or impose a reflecting boundary and return to $X > 0$. Hitting the $X = 0$ boundary in (4) is again equivalent to hitting the $F = 0$ boundary in the original CEV process (1), so appropriate boundary conditions must also be applied at the origin for that process in the regime $\alpha < 0.5$.

4.2.1. *Absorbing boundary*

The unique fundamental solution assuming an *absorbing* boundary condition is given by (11). Accordingly, all paths will eventually be trapped at the origin as in the $\delta \le 0$ case.

As for that case, probability mass is present at the origin, and the full norm-preserving transition density is given by (14). This equation is thus valid for $\delta < 2$, with an absorbing boundary at $X = 0$.

4.2.2. *Reflecting boundary*

Feller does not derive the corresponding solution given a *reflecting* boundary condition, but by imposing a zero flux at $X = 0$, it is relatively easy to show[4] that the transition density is

$$p_\delta(X_T, T; X_0) = \frac{1}{2T}\left(\frac{X_T}{X_0}\right)^{\nu/2} \exp\left[-\frac{(X_T + X_0)}{2T}\right] I_\nu\left(\frac{\sqrt{X_T X_0}}{T}\right), \tag{19}$$

and that it is norm-preserving:

$$\int_0^\infty p_\delta(X, T; X_0)\,\mathrm{d}X = 1. \tag{20}$$

The only difference between this and (11) is the sign of the order of the Bessel function, but in this case the density function is that of the non-central chi-squared distribution as in (6). We thus have

$$\Pr\left(X \le X_T \middle| X_0\right) = \int_0^{X_T} p_\delta(X, T; X_0)\,\mathrm{d}X = \chi'^2\left(\frac{X_T}{T};\, \delta,\, \frac{X_0}{T}\right). \tag{21}$$

We also note that $p_\delta(X_T, T; X_0) = \mathcal{O}(X_T^\nu)$ as $X_T \to 0$. Since $-1 < \nu < 0$, the transition density (19) is not finite at $X_T = 0$ although its expectation *is*, since $\mathbb{E}[X_T] = \mathcal{O}(X_T^{1+\nu})$ as $X_T \to 0$. In terms of the squared Bessel process (4), this indicates that paths have a propensity towards the vicinity of the origin.

4.3. *The case $\delta > 2$*

Finally when $\delta > 2$, or equivalently $\alpha > 1$, a unique norm-preserving solution exists only when a vanishing flux is present at the $X = 0$ boundary. In this scenario, the process never hits $X = 0$, and boundary conditions cannot be imposed. This fact is well-known in the context of the squared Bessel process, for which X will never hit the origin if $\delta \ge 3$.

From the point of view of the original CEV process, however, this is a statement about the $F = \infty$ boundary and indicates that solutions of (1) remain finite for all time[5]. On the other hand, the Feller test for explosions (see, *e.g.*, [22, 24]) shows that X will never become unbounded in finite time if $\delta > 2$. The origin in the original process is thus also not accessible (as in the limiting $\alpha = 1$ lognormal case).

The transition density for $\delta > 2$ is given by (19). As in the case of $0 < \delta < 2$ with $X = 0$ reflecting, X has a natural representation in terms of the non-central chi-squared distribution, as in (21), but in this case $p_\delta \to 0$ as $X_T \to 0$, paths being pushed away from the origin.

[4] Take equation (3.9) of [15], set $f(t) = 0$, and invert the resulting reduced Laplace transform.

[5] This is in contrast to the deterministic case $\mathrm{d}x = x^\alpha \mathrm{d}t$ which is guaranteed to blow-up in finite time whenever $x(0) > 0$ and $\alpha > 1$.

For the CIR and Heston models, as in (7), a reflecting boundary when $0 < \delta < 2$ is the most natural choice and, as we have already discussed, the $\delta \leq 0$ regime is not generally of interest in these models. The process does then generically admit a representation in terms of a non-central chi-squared distribution, as in (21). Since these models are well-developed, we shall concentrate instead on the absorbing case.

4.4. *Symmetry of the transition density*

If we choose *absorbing* boundary conditions at $X = 0$ when appropriate, then the norm-decreasing part of the transition density is given by (11) for all $\delta < 2$. On the other hand, for $\delta > 2$, the density is given by (19). It is straightforward to verify the following symmetry between these two expressions.

If $\delta < 2$ ($\delta > 2$) then, for $\delta > 2$ ($\delta < 2$), we have

$$p_\delta(X_T, T; X_0) = p_{4-\delta}(X_0, T; X_T). \tag{22}$$

The boundary case at $\delta = 2$ corresponds to $\alpha = 1$, and so there is a similar symmetry relation over $\alpha \to 2 - \alpha$. This feature can be used to generate the density for $\alpha > 1$ ($\alpha < 1$) from that for $\alpha < 1$ ($\alpha > 1$), although one must be careful to (re-)include the Dirac mass in (14) when appropriate. Moreover, for all $\alpha \neq 1$, we have the representation, as in [3]:

$$p_\delta(X_T, T; X_0) = \frac{1}{2T}\left(\frac{X_T}{X_0}\right)^{\nu/2} \exp\left[-\frac{X_T + X_0}{2T}\right] I_{|\nu|}\left(\frac{\sqrt{X_T X_0}}{T}\right). \tag{23}$$

The literature has often used the identity $I_\nu(z) = I_{-\nu}(z)$ for integer ν to extend the results for $\delta < 2$ to the case $\delta > 2$. However, this is not typically valid and indeed not required. The symmetry (22) is simply true by a direct calculation of the densities in the two regimes, with an absorbing boundary where appropriate.

5. EXPECTATION AND VARIANCE OF X

In this section, we derive expressions for the mean and expectation of the squared Bessel process (4) based on the transition densities developed in sections §4.1-§4.3. These quantities are derived directly from the Fokker-Planck equation (8). The results derived here are verified using Monte Carlo simulation in §8.

First, the expected value

$$\mathbb{E}\left[X_T | X_0\right] \equiv \mu_X = \int_0^\infty X p_\delta^{\text{full}}(X, T; X_0)\,\mathrm{d}X = \int_0^\infty X\, p_\delta(X, T; X_0)\,\mathrm{d}X,$$

where the Dirac mass in (14) vanishes, so we can safely calculate the expected value directly from (8a). Multiplying the latter by X and integrating by parts gives

$$\frac{\partial \mu_X}{\partial t} = \lim_{X \to 0}\left[X f(t) + 2Xp\right] + \delta \int_0^\infty p_\delta(X, T; X_0)\,\mathrm{d}X,$$

where the flux, $f(t)$, at the origin is given by expression (9). For all δ, the first term on the right hand side vanishes, giving the ordinary differential equation (ODE) for μ_X:

$$\frac{\partial \mu_X}{\partial t} = \delta \int_0^\infty p_\delta(X, T; X_0)\,\mathrm{d}X, \qquad t > 0; \qquad \mu_X(0) = X_0. \tag{24}$$

The expected value is either strictly increasing or strictly decreasing depending on the sign of δ.

To calculate the variance, we first note that

$$\begin{aligned} \mathrm{Var}\,[\,X_T|\,X_0] \equiv \sigma_X^2 &= \int_0^\infty (X-\mu_X)^2\; p_\delta^{\mathrm{full}}(X,T;X_0)\,\mathrm{d}X \\ &= \int_0^\infty X^2\, p_\delta(X,T;X_0)\,\mathrm{d}X - \mu_X^2 \\ &\equiv \bar{\sigma}_X^2 - \mu_X^2, \end{aligned}$$

where again the Dirac mass in (14) vanishes, and seek an ODE for $\bar{\sigma}_X^2$ by multiplying equation (8a) by X^2 followed by integrating by parts. As for the expected value, the contribution to the integral from the boundary $X = 0$ is zero and so we obtain that $\bar{\sigma}_X^2$ satisfies

$$\frac{\partial \bar{\sigma}_X^2}{\partial t} = 2\,\mu_X(2+\delta), \qquad t > 0; \qquad \bar{\sigma}_X^2(0) = X_0^2. \tag{25}$$

To develop solutions of (24) and (25), two separate cases are considered.

5.1. *The norm-preserving case*

For $\delta > 2$, and for $0 < \delta < 2$ with a *reflecting* boundary at the origin, the transition density is norm-preserving, so that the solution of (24) is

$$\mu_X = X_0 + \delta\, T. \tag{26}$$

The solution of equation (25) is straightforward and gives

$$\sigma_X^2 = 2\,\delta\,T^2 + 4X_0\,T.$$

These are standard results for the non-central chi-squared distribution.

5.2. *The norm-decreasing case*

For $\delta < 0$, and for $0 < \delta < 2$ with an *absorbing* boundary condition at the origin, the transition density is defective. As shown in Appendix A, integrating (24) by parts reveals that

$$\mu_X = [X_0 + \delta\,T]\;\Gamma\left(-\nu; \frac{X_0}{2T}\right) + \frac{X_0}{\Gamma(-\nu)}\left(\frac{X_0}{2T}\right)^{-\nu-1} e^{-X_0/2T}, \tag{27}$$

and that $\sigma_X^2 = \bar{\sigma}_X^2 - \mu_X^2$ where

$$\begin{aligned}\bar{\sigma}_X^2 = \left[\delta(2+\delta)\,T^2 + 2X_0(2+\delta)\,T + X_0^2\right]\Gamma\left(-\nu;\frac{X_0}{2T}\right) \\ + \left[\delta T + X_0 + 4T\right]\frac{2T}{\Gamma(-\nu)}\left(\frac{X_0}{2T}\right)^{-\nu} e^{-\frac{X_0}{2T}}.\end{aligned} \tag{28}$$

6. EXPECTED VALUE OF F, AND THE LOCAL MARTINGALE PROPERTY

Here, we derive expressions for the mean of the original CEV process (1) based on the results developed in sections §4.1-§4.4. We assume an absorbing boundary at the origin in the $0 < \delta < 2$ regime.

For any δ, the expectation of F_T is

$$\mathbb{E}\left[F_T \mid F_0\right] \equiv \mu_F = \sigma^{-2\nu}(1-\alpha)^{-2\nu}\int_0^\infty X^{-\nu}\, p_\delta(X,T;X_0)\,\mathrm{d}X,$$

(where for $\delta < 2$, the Dirac mass vanishes from the integral of p_δ^{full}). Substitution of (11) or (19), and using the symmetry (22), gives

$$X^{-\nu}p_\delta(X,T;X_0) = X_0^{-\nu}p_\delta(X_0,T;X) = X_0^{-\nu}p_{4-\delta}(X,T;X_0),$$

so that

$$\mu_F = F_0\int_0^\infty p_{4-\delta}(X,T;X_0)\,\mathrm{d}X.$$

For $\delta < 2$, this integral is norm-preserving, making F a martingale as expected. However, for $\delta > 2$, the integral is norm-decreasing, so that F is a *strictly local martingale*[6]:

$$\mu_F = F_0\,\Gamma\left(-\nu;\frac{X_0}{2T}\right) < F_0. \tag{29}$$

As discussed by Lewis [23], the CEV process (1) with $\alpha > 1$ is such that the forward price is only a local martingale. The amount by which it differs from a true martingale is shown in Figure 2; and these results are verified using Monte Carlo simulation in §8.

The fact that F is a strictly local martingale when $\alpha > 1$ is not necessarily pertinent when the CEV process is considered in a financial setting, as such discussions typically concentrate on the $\alpha < 1$ regime. Moreover, as can be seen from Figure 2, one has to take fairly large values of α to see a significant deviation from the martingale property. Nevertheless, the effect is an important one, and we shall observe in the following section that the prices of plain vanilla European call options are sensitive to this effect.

[6] A rigorous definition of a strictly local martingale is given in, *e.g.*, [22]. For our purposes, however, if will suffice to take a local martingale to be a process $\mathrm{d}F = \sigma(F,t)\,\mathrm{d}W$ with $\mathbb{E}[F_T \mid F_0] < F_0$.

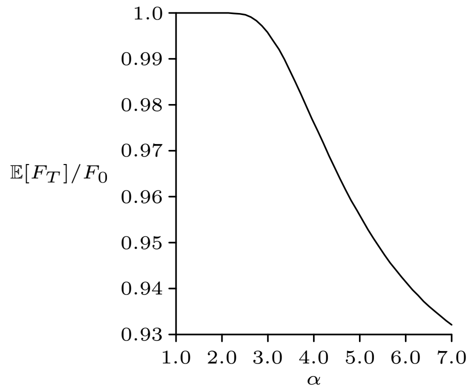

FIGURE 2.— Plot of $\mathbb{E}[F_T]/F_0$ against $\alpha > 1$ for parameter values $F_0 = 100$, $T = 1$, $\sigma_{\mathrm{LN}} = 0.2$.

7. CLOSED-FORM PLAIN VANILLA OPTION PRICES

Here we derive the prices of plain vanilla European options, based on the results developed in sections §4.1-§4.4. We compute the European call price explicitly, and derive the put price from put-call parity. We again assume an absorbing boundary at the origin in the $0 < \delta < 2$ regime.

The forward, or at-expiry, price of a plain vanilla European call option is

$$C = \mathbb{E}\left[\max\left(F_T - K, 0\right)\middle|\, F_0\right] = \int_K^\infty (F - K)\; p(F, T; F_0)\,\mathrm{d}F,$$

where K is the strike price of the option, which maturity T.

The forward price of the corresponding put option can be found through put-call parity:

$$P = C - \mathbb{E}\left[F_T - K\middle|\, F_0\right] = C - \mathbb{E}\left[F_T\middle|\, F_0\right] - K, \tag{30}$$

where in general (if F_T is only a local martingale), the right-hand side is *not* equal to $C - F_0 - K$.

Once we transform to the X coordinate, we need to differentiate between the $\delta < 2$ and $\delta > 2$ regimes.

7.1. *The case* $\delta < 2$

For $\delta < 2$, or $\alpha < 1$, we have

$$C_{\delta<2} = \int_{\tilde{K}}^\infty \left[\frac{X^{-\nu}}{\left(\sigma(1-\alpha)\right)^{2\nu}} - K\right] p_\delta^{\mathrm{full}}(X, T; X_0)\,\mathrm{d}X, \tag{31}$$

where

$$\tilde{K} = \frac{K^{2(1-\alpha)}}{\sigma^2 (1-\alpha)^2}, \tag{32}$$

and p_δ^{full} is the full norm-preserving transition density given by (14). From (18), the second integral in (31) is

$$\int_{\tilde{K}}^{\infty} p_\delta^{\text{full}}(X, T; X_0)\, \mathrm{d}X = {\chi'}^2\left(\frac{X_0}{T}; 2-\delta, \frac{\tilde{K}}{T}\right).$$

The Dirac mass vanishes from the first integral, and after applying the symmetry (22), we have

$$C_{\delta<2} = F_0\left[1 - {\chi'}^2\left(\frac{\tilde{K}}{T}; 4-\delta, \frac{X_0}{T}\right)\right] - K{\chi'}^2\left(\frac{X_0}{T}; 2-\delta, \frac{\tilde{K}}{T}\right). \tag{33}$$

From (30), the corresponding put price is

$$\begin{aligned} P_{\delta<2} &= C_{\delta<2} + K - F_0 \\ &= K\left[1 - {\chi'}^2\left(\frac{X_0}{T}; 2-\delta, \frac{X_T}{T}\right)\right] - F_0{\chi'}^2\left(\frac{\tilde{K}}{T}; 4-\delta, \frac{X_0}{T}\right). \end{aligned} \tag{34}$$

These expressions agree with [27].

7.2. *The case $\delta > 2$*

For $\delta > 2$, or $\alpha > 1$, we have

$$C_{\delta>2} = \int_0^{\tilde{K}} \left[\frac{X^{-\nu}}{(\sigma(1-\alpha))^{2\nu}} - K\right] p_\delta(X, T; X_0)\, \mathrm{d}X,$$

where the relevant (norm-preserving) transition density is given by (19). The second integral is a cumulative non-central chi-squared distribution, but the first integral becomes

$$F_0 \int_0^{\tilde{K}} p_{4-\delta}(X, T; X_0)\, \mathrm{d}X,$$

upon use of the symmetry (22). Since $\delta > 2$, the transition density $p_{4-\delta}$ is the norm-decreasing density given in (11) and, from (17), we have

$$C_{\delta>2} = F_0\left[\Gamma\left(\nu; \frac{X_0}{2T}\right) - {\chi'}^2\left(\frac{X_0}{T}; \delta-2, \frac{X_T}{T}\right)\right] - K{\chi'}^2\left(\frac{\tilde{K}}{T}; \delta, \frac{X_0}{T}\right). \tag{35}$$

From (30), the corresponding put price is

$$
\begin{aligned}
P_{\delta>2} &= C_{\delta>2} + K - F_0\,\Gamma\left(-\nu; \frac{X_0}{2T}\right) \\
&= K\left[1 - {\chi'}^2\left(\frac{\tilde{K}}{T};\, \delta,\, \frac{X_0}{T}\right)\right] - F_0 {\chi'}^2\left(\frac{X_0}{T}; \delta - 2, \frac{X_T}{T}\right).
\end{aligned} \tag{36}
$$

The expression (35) for $C_{\delta>2}$ agrees with Lewis [23], and as he has pointed out, it is *not* the same as that widely reported in the literature (see, *e.g.*, [20], the origin of this being attributed to [14] in [27]). The standard result has the $F_0\Gamma(\nu; X_0/(2T))$ term in (35) replaced with F_0. Lewis writes the call price as $\mathbb{E}[\max(S_T - K, 0)] + F_0\Gamma(\nu; X_0/(2T))$, but this does not appear to be correct either; the call price is precisely $\mathbb{E}[\max(S_T - K, 0)]$, as should be expected, but one must be careful about the transitional density used in the calculation of the expected value.

On the other hand, the put price (36), does agree with that in the literature, but only by a cancellation of errors: the replacement of $F_0\Gamma(\nu; X_0/(2T))$ with F_0 in (35) is canceled out by the mistaken assumption that F_T is a martingale.

8. MONTE CARLO SIMULATION

In this section, we perform an exact simulation of the squared Bessel and CEV processes, and compute both the forward prices $\mathbb{E}[X_T]$ and $\mathbb{E}[F_T]$, as well as plain vanilla European prices. We find good agreement with the analytic results obtained above.

We actually perform *quasi*-Monte Carlo simulations, using the Sobol sequence of numbers (see, *e.g.*, [16] for an overview of these techniques). Given N samples of $X_T^{(i)}$, the expectation value is just the mean

$$
\mathbb{E}[X_T] \approx \frac{1}{N}\sum_{i=1}^{N} X_T^{(i)},
$$

the error in this approximation being of $\mathcal{O}(\log N/N)$ for quasi-Monte Carlo simulations. We always sample X_T, and obtain F_T through inversion of (3). We assume an absorbing boundary where appropriate, and always take $N = 2^{20} - 1$ in our simulations[7].

8.1. *The case $\delta < 2$*

For $\delta < 2$, or $\alpha < 1$, the full transition density (14) consists of the norm-decreasing density (19) and a Dirac mass at the origin.

[7]For quasi-Monte Carlo simulations with the Sobol sequence of numbers, one should use $2^n - 1$ paths, with n an integer, so that the mean of the set of numbers used is precisely equal to 0.5.

To simulate X_T, one might think to sample directly from the distribution given in (18). Drawing numbers $U = \Pr\left(X \leq X_T | \, X_0 \right) \in (0,1)$ from a uniform distribution, one would have

$$\chi'^2\left(\frac{X_0}{T}; 2-\delta, \frac{X_T}{T}\right) = 1 - U, \tag{37}$$

so X_T/T would be the formal inverse of the non-central chi-squared distribution as a function of the non-centrality parameter: with $\mathcal{F}(x) \equiv \chi'^2(X_0/T; 2-\delta, x)$, we would have

$$\frac{X_T}{T} = \mathcal{F}^{-1}\left(1 - U\right).$$

However, accounting for the absorption at $X = 0$ that this distribution captures is difficult numerically; there are many values of U for which $X_T = 0$ is the correct solution.

It is more straightforward to account for the absorption "by hand" as it were. We draw numbers $U \in (0,1)$ from a uniform distribution. Then, if

$$U > U_{\max} \equiv \Gamma\left(-\nu; \frac{X_0}{2T}\right),$$

we simply set $X_T = 0$. On the other hand, if $U \leq U_{\max}$, then we sample from the norm-decreasing density (11) by inverting the integral (17) to obtain

$$\frac{X_T}{T} = \mathcal{F}^{-1}\left(U_{\max} - U\right).$$

To compute this numerically, we perform a root search over values of X_T. For each such value, we construct a *new* cumulative non-central chi-squared distribution, which is nevertheless always evaluated at the point X_0/T. As mentioned above, we use a variation of the algorithm in [10] to perform all such evaluations of chi-squared distributions.

We compare the simulated values of $\mathbb{E}[X_T]$ with (27), and those of $\mathbb{E}[F_T]$ with F_0. Table II gives some results of the simulation of $\mathbb{E}[X_T]$ for selected values of α, in which we have taken $F_0 = 100$, $\sigma_{\text{LN}} = 50\%$ and $T = 4$ (we take both σ_{LN} and T to be relatively large so that the amount by which $U_{\max}$ differs from unity is large enough to test our simulation method properly). The 1-sigma confidence intervals of the simulated results are also given, and the agreement is very good.

The simulated values of European call and put prices are compared with (33) and (34) respectively. We again find good agreement, as shown for selected values of α in Table III, in which we have again taken $F_0 = 100$, $\sigma_{\text{LN}} = 50\%$, $T = 4$ and have calculated option prices for $K = 90, 100, 110$.

α	Simulated	Analytic
-2	5.53758 ± 0.00769	5.53767
-1	5.63895 ± 0.00800	5.63894
0	7.39724 ± 0.00981	7.39728
0.1	8.01965 ± 0.01034	8.01988
0.2	8.91106 ± 0.01106	8.91104
0.3	10.24398 ± 0.01204	10.24398
0.4	12.35917 ± 0.01347	12.35922
0.5	15.99998 ± 0.01562	16.00000
0.6	23.02961 ± 0.01910	23.02969
0.7	39.12362 ± 0.02523	39.12283
0.8	88.00108 ± 0.03787	88.00013
0.9	367.9997 ± 0.07655	368.00000

TABLE II
Simulated and analytic values of $\mathbb{E}[X_T]$ for $\alpha < 1$, $F_0 = 100$, $\sigma_{\text{LN}} = 50\%$ and $T = 4$

8.2. *The case* $\delta > 2$

For $\delta > 2$, or $\alpha > 1$, the variable X_T can be simulated by sampling from a non-central chi-squared distribution directly, as in (21). This can be done in various ways (see, *e.g.* [16]). The simplest method, and the one we choose here, is to draw numbers $U = \Pr(X \le X_T | X_0) \in (0,1)$ from a uniform distribution, and invert (21) directly to give

$$\frac{X_T}{T} = \chi'^{\,-1}\left(U; \delta, \frac{X_0}{T}\right),$$

where $\chi'^{\,-1}(x; k, \lambda)$ denotes the inverse cumulative non-central chi-squared distribution, with k degrees of freedom and non-centrality parameter λ.

The inversion of the non-central chi-squared distribution is again performed using a root search over the cumulative non-central chi-squared distribution. Although computationally expensive, this method will suffice for our purposes. An alternative would be to use the quadratic-exponential method described by Andersen [2].

We compare the simulated values of $\mathbb{E}[X_T]$ and $\mathbb{E}[F_T]$ with (26) and (29) respectively, and find good agreement. In particular, the latter comparison confirms that F_T is a strictly local martingale when $\alpha > 1$: a plot of the simulated value of $\mathbb{E}[F_T]$ would show no difference to the analytic result in Figure 2. Table IV gives some results for the simulation of $\mathbb{E}[F_T]$ for selected values of α, in which we have taken $F_0 = 100$, $\sigma_{\text{LN}} = 20\%$ and $T = 1$. The 1-sigma confidence intervals of the simulated results are also given, and the agreement is very good.

The simulated values of European call and put prices are compared with (35) and (36) respectively. We again find good agreement, as shown for selected values of α in Table V, in which we have again taken $F_0 = 100$, $\sigma_{\text{LN}} = 20\%$, $T = 1$ and have calculated option prices for $K = 90, 100, 110$. We also include the standard

	Call $K = 90$		Put $K = 90$	
α	Simulated	Analytic	Simulated	Analytic
-2	40.78006 ± 0.03638	40.78008	30.78005 ± 0.04151	30.78008
-1	43.22328 ± 0.04515	43.22324	33.22319 ± 0.04185	33.22324
0	43.98798 ± 0.06049	43.98810	33.98807 ± 0.03986	33.98810
0.1	43.81498 ± 0.06278	43.81494	33.81489 ± 0.03923	33.81494
0.2	43.58713 ± 0.06531	43.58722	33.58719 ± 0.03844	33.58722
0.3	43.31549 ± 0.06815	43.31579	33.31577 ± 0.03748	33.31579
0.4	43.02014 ± 0.07138	43.02028	33.02024 ± 0.03634	33.02028
0.5	43.02014 ± 0.07138	43.02028	33.02024 ± 0.03634	33.02028
0.6	42.44313 ± 0.07951	42.44328	32.44324 ± 0.03369	32.44328
0.7	42.18646 ± 0.08485	42.18694	32.18690 ± 0.03235	32.18694
0.8	41.95756 ± 0.09165	41.95539	31.95529 ± 0.03108	31.95539
0.9	41.74670 ± 0.10064	41.74895	31.74894 ± 0.02987	31.74895

	Call $K = 100$		Put $K = 100$	
α	Simulated	Analytic	Simulated	Analytic
-2	34.42926 ± 0.03259	34.42928	34.42925 ± 0.04602	34.42928
-1	37.38754 ± 0.04146	37.38750	37.38744 ± 0.04630	37.38750
0	39.04504 ± 0.05709	39.04516	39.04513 ± 0.04396	39.04516
0.1	39.00895 ± 0.05943	39.00891	39.00885 ± 0.04327	39.00891
0.2	38.93068 ± 0.06202	38.93077	38.93073 ± 0.04242	38.93077
0.3	38.82058 ± 0.06492	38.82088	38.82086 ± 0.04139	38.82088
0.4	38.69621 ± 0.06822	38.69635	38.69630 ± 0.04019	38.69635
0.5	38.57511 ± 0.07203	38.57528	38.57523 ± 0.03886	38.57528
0.6	38.47236 ± 0.07653	38.47251	38.47246 ± 0.03746	38.47251
0.7	38.39167 ± 0.08199	38.39215	38.39212 ± 0.03608	38.39215
0.8	38.33770 ± 0.08895	38.33554	38.33544 ± 0.03476	38.33554
0.9	38.30141 ± 0.09812	38.30366	38.30365 ± 0.03350	38.30366

	Call $K = 110$		Put $K = 110$	
α	Simulated	Analytic	Simulated	Analytic
-2	28.28012 ± 0.02884	28.28014	38.28011 ± 0.05044	38.28014
-1	31.81090 ± 0.03779	31.81087	41.81080 ± 0.05064	41.81087
0	34.44658 ± 0.05368	34.44670	44.44667 ± 0.04794	44.44670
0.1	34.55394 ± 0.05606	34.55391	44.55384 ± 0.04719	44.55391
0.2	34.62999 ± 0.05871	34.63008	44.63004 ± 0.04628	44.63008
0.3	34.68399 ± 0.06167	34.68429	44.68427 ± 0.04519	44.68429
0.4	34.73096 ± 0.06505	34.73110	44.73106 ± 0.04394	44.73110
0.5	34.78481 ± 0.06895	34.78498	44.78493 ± 0.04255	44.78498
0.6	34.85746 ± 0.07356	34.85761	44.85756 ± 0.04111	44.85761
0.7	34.95133 ± 0.07915	34.95181	44.95177 ± 0.03968	44.95181
0.8	35.07131 ± 0.08626	35.06915	45.06904 ± 0.03830	45.06915
0.9	35.20904 ± 0.09563	35.21129	45.21128 ± 0.03698	45.21129

TABLE III

Simulated and analytic values of call and put prices for $\alpha < 1$, $F_0 = 100$, $\sigma_{\mathrm{LN}} = 50\%$ and $T = 4$

α	Simulated	Analytic
1.5	1.00000 ± 0.00020	1.00000
2	0.99999 ± 0.00021	1.00000
2.5	0.99957 ± 0.00022	0.99958
3	0.99568 ± 0.00022	0.99569
3.5	0.98701 ± 0.00021	0.98701
4	0.97612 ± 0.00018	0.97612
4.5	0.96537 ± 0.00016	0.96537
5	0.95586 ± 0.00014	0.95586
5.5	0.94789 ± 0.00013	0.94789
6	0.94140 ± 0.00012	0.94140
6.5	0.93621 ± 0.00011	0.93621
7	0.93210 ± 0.00010	0.93210

TABLE IV
Simulated and analytic values of $\mathbb{E}[F_T]/F_0$ for $\alpha > 1$, $F_0 = 100$, $\sigma_{\mathrm{LN}} = 20\%$ and $T = 1$

call option prices, which are clearly incorrect, although one has to go to fairly large values of α to see the discrepancy.

9. Conclusion

We have given a clear overview of the CEV process (1), discussing the Feller classification of boundary conditions and associated probability transition functions, according to the value of the CEV exponent α. Since the transition density of the squared Bessel process is norm-decreasing in the $\delta \leq 0$ regime (and also, given an absorbing boundary condition, in the $0 < \delta < 2$ regime), we have argued that it should be amended with a Dirac mass at the origin, with strength such that the resulting full transition density is norm-preserving. The cumulative distribution in this case is related to the non-central chi-squared distribution, but as a function of non-centrality parameter.

We have noted a symmetry between the transition densities in the two regimes $\delta < 2$ (with absorbing boundary conditions where appropriate) and $\delta > 2$, which readily explains various results. In particular, one can use the symmetry to show that the forward price is a strictly local martingale when $\alpha > 1$. We have further argued that the standard European call price for $\alpha > 1$ requires a correction, and have shown how this is naturally included in a direct calculation of the expectation value of the option payoff.

Monte Carlo simulation of the CEV process has been discussed, in particular a new scheme has been given to simulate the forward price when $\alpha < 1$, which accounts for the probability of absorption at the origin. We used these techniques to simulate the expectation values, both of X and F, and of European option prices, and compared them to the analytic results. The agreement is extremely good.

	Call $K = 90$			Put $K = 90$	
α	Simulated	Analytic	Standard	Simulated	Analytic
1.5	13.42092 ± 0.01677	13.42112	13.42105	3.42103 ± 0.00614	3.42105
2	13.26095 ± 0.01804	13.26142	13.26149	3.26147 ± 0.00568	3.26149
2.5	13.06691 ± 0.01995	13.06792	13.10955	3.10953 ± 0.00528	3.10955
3	12.53248 ± 0.02019	12.53325	12.96456	2.96455 ± 0.00491	2.96456
3.5	11.52695 ± 0.01850	11.52768	12.82609	2.82608 ± 0.00459	2.82609
4	10.30586 ± 0.01628	10.30592	12.69389	2.69388 ± 0.00429	2.69389
4.5	9.10458 ± 0.01420	9.10488	12.56774	2.56773 ± 0.00402	2.56774
5	8.03280 ± 0.01244	8.03275	12.44701	2.44700 ± 0.00377	2.44701
5.5	7.11956 ± 0.01099	7.12023	12.33066	2.33065 ± 0.00354	2.33066
6	6.35763 ± 0.00980	6.35740	12.21751	2.21751 ± 0.00333	2.21751
6.5	5.72731 ± 0.00883	5.72697	12.10663	2.10663 ± 0.00313	2.10663
7	5.20693 ± 0.00803	5.20782	11.99741	1.99740 ± 0.00295	1.99741

	Call $K = 100$			Put $K = 100$	
α	Simulated	Analytic	Standard	Simulated	Analytic
1.5	7.96872 ± 0.01385	7.96887	7.96885	7.96883 ± 0.00967	7.96885
2	7.96872 ± 0.01528	7.97879	7.97885	7.97883 ± 0.00924	7.97885
2.5	7.95335 ± 0.01742	7.95453	7.99598	7.99597 ± 0.00885	7.99598
3	7.95335 ± 0.01773	7.58979	8.02115	8.02113 ± 0.00849	8.02115
3.5	6.75691 ± 0.01597	6.75739	8.05605	8.05604 ± 0.00815	8.05605
4	5.71528 ± 0.01366	5.71516	8.10331	8.10330 ± 0.00783	8.10331
4.5	4.70077 ± 0.01151	4.70092	8.16394	8.16393 ± 0.00753	8.16394
5	3.82032 ± 0.00970	3.82051	8.23453	8.23453 ± 0.00723	8.23453
5.5	3.09733 ± 0.00822	3.09681	8.30843	8.30842 ± 0.00695	8.30843
6	2.51872 ± 0.00702	2.51885	8.37860	8.37860 ± 0.00667	8.37860
6.5	2.06033 ± 0.00605	2.06009	8.43965	8.43964 ± 0.00641	8.43965
7	1.69776 ± 0.00525	1.69846	8.48825	8.48824 ± 0.00616	8.48825

	Call $K = 110$			Put $K = 110$	
α	Simulated	Analytic	Standard	Simulated	Analytic
1.5	4.47417 ± 0.01083	4.47428	4.47430	14.47428 ± 0.01287	14.47430
2	4.66758 ± 0.01247	4.66790	4.66812	14.66811 ± 0.01242	14.66812
2.5	4.83321 ± 0.01491	4.83459	4.87584	14.87583 ± 0.01199	14.87584
3	4.66904 ± 0.01530	4.67006	5.10113	15.10111 ± 0.01157	15.10113
3.5	4.05128 ± 0.01350	4.05159	5.35042	15.35041 ± 0.01115	15.35042
4	3.24321 ± 0.01117	3.24310	5.63124	15.63123 ± 0.01072	15.63124
4.5	2.47823 ± 0.00904	2.47753	5.94139	15.94139 ± 0.01026	15.94139
5	1.85077 ± 0.00729	1.85091	6.26497	16.26497 ± 0.00979	16.26497
5.5	1.37029 ± 0.00589	1.37029	6.58138	16.58138 ± 0.00932	16.58138
6	1.01409 ± 0.00479	1.01430	6.87397	16.87396 ± 0.00886	16.87397
6.5	0.75351 ± 0.00393	0.75357	7.13283	17.13282 ± 0.00841	17.13283
7	0.56346 ± 0.00325	0.56388	7.35394	17.35394 ± 0.00799	17.35394

TABLE V

Simulated and analytic values of call and put prices for $\alpha > 1$, $F_0 = 100$, $\sigma_{\mathrm{LN}} = 20\%$ and $T = 1$

In particular, for $\alpha > 1$, the simulated results show that the forward price in the CEV model is indeed a local martingale, and agree with the corrected call price. The $\alpha > 1$ regime is not often discussed in the literature and at any rate, fairly large values of α must be considered to see these results. But they are nevertheless significant.

APPENDIX A: MEAN AND VARIANCE OF X

To calculate μ_X, integrate (24) over $[0, T]$ to get

$$\mu_X(T) = X_0 + \delta \int_0^T \Gamma\left(-\nu; \frac{X_0}{2t}\right) \mathrm{d}t.$$

Integrating this expression by parts, it follows that

$$\begin{aligned}
\int_0^T \Gamma\left(-\nu; \frac{X_0}{2t}\right) \mathrm{d}t &= t\,\Gamma\left(-\nu; \frac{X_0}{2t}\right)\Big|_{t=0}^{t=T} + \frac{1}{\Gamma(-\nu)} \int_0^T \left(\frac{X_0}{2t}\right)^{-\nu} e^{-\frac{X_0}{2t}} \mathrm{d}t \\
&= T\,\Gamma\left(-\nu; \frac{X_0}{2T}\right) + \frac{X_0}{2\Gamma(-\nu)} \int_{X_0/2T}^{\infty} y^{-\nu-2} e^{-y} \mathrm{d}y \\
&= T\,\Gamma\left(-\nu; \frac{X_0}{2T}\right) + \frac{X_0}{2(\nu+1)\Gamma(-\nu)} \left(\frac{X_0}{2T}\right)^{-\nu-1} e^{-X_0/2T} \\
&\quad - \frac{X_0}{2(\nu+1)} \left[1 - \Gamma\left(-\nu; \frac{X_0}{2T}\right)\right].
\end{aligned}$$

Now with $\nu = \delta/2 - 1$, $\mu_X(T)$ is determined to be

$$\mu_X(T) = [X_0 + \delta\,T]\Gamma\left(-\nu; \frac{X_0}{2T}\right) + \frac{X_0}{\Gamma(-\nu)} \left(\frac{X_0}{2T}\right)^{-\nu-1} e^{-X_0/2T}.$$

The variance satisfies $\sigma_X^2 = \bar{\sigma}_X^2 - \mu_X^2$, where is $\bar{\sigma}_X^2$ is defined in equation (25). Integrating this quantity we have that

$$\begin{aligned}
\bar{\sigma}_X^2(T) &= X_0^2 + 2(2+\delta) \int_0^T \mu_X(t)\,\mathrm{d}t \\
&= X_0^2 + 2(2+\delta) \left[X_0 \int_0^T \Gamma\left(-\nu; \frac{X_0}{2t}\right) \mathrm{d}t + \delta \int_0^T t\,\Gamma\left(-\nu; \frac{X_0}{2t}\right) \mathrm{d}t \right. \\
&\quad \left. + \frac{X_0}{\Gamma(-\nu)} \int_0^t \left(\frac{X_0}{2t}\right)^{-\nu-1} e^{-\frac{X_0}{2t}} \mathrm{d}t\right] \\
&\equiv X_0^2 + 2(2+\delta) \left[X_0\, I_1 + \delta\, I_2 + \frac{X_0}{\Gamma(-\nu)} I_3\right].
\end{aligned}$$

The integral I_1 has been determined previously in the calculation for μ_X as

$$\begin{aligned}
I_1 &\equiv \int_0^T \Gamma\left(-\nu; \frac{X_0}{2t}\right) \mathrm{d}t \\
&= T\,\Gamma\left(-\nu; \frac{X_0}{2T}\right) + \frac{X_0}{2(\nu+1)} \left[\frac{1}{\Gamma(-\nu)} \left(\frac{X_0}{2T}\right)^{-\nu-1} e^{-\frac{X_0}{2T}} - 1 + \Gamma\left(-\nu; \frac{X_0}{2T}\right)\right].
\end{aligned}$$

The calculation of I_2 proceeds as follows

$$\begin{aligned}
I_2 &\equiv \int_0^T t\,\Gamma\left(-\nu; \frac{X_0}{2t}\right) \mathrm{d}t \\
&= \frac{T^2}{2}\Gamma\left(-\nu; \frac{X_0}{2T}\right) + \frac{X_0}{4\Gamma(-\nu)} \int_0^T \left(\frac{X_0}{2t}\right)^{-\nu-1} e^{-\frac{X_0}{2t}}\,\mathrm{d}t \\
&= \frac{T^2}{2}\Gamma\left(-\nu; \frac{X_0}{2T}\right) + \frac{X_0^2}{8\Gamma(-\nu)} \int_{\frac{X_0}{2T}}^\infty y^{-\nu-3} e^{-y}\,\mathrm{d}y \\
&= \frac{T^2}{2}\Gamma\left(-\nu; \frac{X_0}{2T}\right) + \frac{X_0^2}{8(\nu+2)\Gamma(-\nu)} \left[\left(\frac{X_0}{2T}\right)^{-\nu-2} e^{-\frac{X_0}{2T}} - \int_{\frac{X_0}{2T}}^\infty y^{-\nu-2} e^{-y}\,\mathrm{d}y\right] \\
&= \frac{T^2}{2}\Gamma\left(-\nu; \frac{X_0}{2T}\right) + \frac{X_0^2}{8(\nu+2)\Gamma(-\nu)} \left[\left(\frac{X_0}{2T}\right)^{-\nu-2} e^{-\frac{X_0}{2T}} - \int_{\frac{X_0}{2T}}^\infty y^{-\nu-2} e^{-y}\,\mathrm{d}y\right] \\
&= \frac{T^2}{2}\Gamma\left(-\nu; \frac{X_0}{2T}\right) + \frac{X_0^2}{8(\nu+2)\Gamma(-\nu)} \left(\frac{X_0}{2T}\right)^{-\nu-2} e^{-\frac{X_0}{2T}} \\
&\quad - \frac{X_0^2}{8(\nu+2)(\nu+1)\Gamma(-\nu)} \left[\left(\frac{X_0}{2T}\right)^{-\nu-1} e^{-\frac{X_0}{2T}} - \Gamma(-\nu)\left[1 - \Gamma\left(-\nu; \frac{X_0}{2T}\right)\right]\right].
\end{aligned}$$

The calculation of I_3 proceeds as follows

$$\begin{aligned}
I_3 &\equiv \int_0^T \left(\frac{X_0}{2t}\right)^{-\nu-1} e^{-\frac{X_0}{2t}}\,\mathrm{d}t \\
&= \frac{X_0}{2} \int_{\frac{X_0}{2T}}^\infty y^{-\nu-3} e^{-y}\,\mathrm{d}y \\
&= \frac{X_0}{2(\nu+2)} \left[\left(\frac{X_0}{2T}\right)^{-\nu-2} e^{-\frac{X_0}{2T}} - \int_{X_0/2T}^\infty y^{-\nu-2} e^{-y}\,\mathrm{d}y\right] \\
&= \frac{X_0}{2(\nu+2)} \left(\frac{X_0}{2T}\right)^{-\nu-2} e^{-\frac{X_0}{2T}} \left[1 - \frac{X_0}{2T(\nu+1)}\right] \\
&\quad + \frac{X_0\Gamma(-\nu)}{2(\nu+1)(\nu+2)} \left[1 - \Gamma\left(-\nu; \frac{X_0}{2T}\right)\right].
\end{aligned}$$

Combining integrals I_1, I_2 and I_3 to calculate $\bar{\sigma}_X^2$, we have that

$$\begin{aligned}
\bar{\sigma}_X^2 &= \left[\delta(2+\delta)\,T^2 + 2X_0(2+\delta)\,T + X_0^2\right]\Gamma\left(-\nu; \frac{X_0}{2T}\right) \\
&\quad + \left[\delta\,T + X_0 + 4T\right] \frac{2T}{\Gamma(-\nu)} \left(\frac{X_0}{2T}\right)^{-\nu} e^{-\frac{X_0}{2T}}.
\end{aligned}$$

REFERENCES

[1] L. Andersen. Credit Explosives. Available at `http://ssrn.com/abstract=262682`, 2001.

[2] L. Andersen. Efficient Simulation of the Heston Stochastic Volatility Model. Available at `http://ssrn.com/abstract=946405`, 2007.

[3] L. Andersen and J. Andreasen. Volatility Skews and Extensions of the Libor Market Model. Available at `http://ssrn.com/abstract=111030`, 1998.

[4] M. Atlan and B. Leblanc. Time-Changed Bessel Processes and Credit Risk. Available at `http://arxiv.org/abs/math.PR/0604305`, 2006.

[5] F. Black and M. Scholes. The Pricing of Options and Corporate Liabilities. *Journal of Political Economy*, 81:637–659, 1973.

[6] J. C. Cox. The Constant Elasticity of Variance Option Pricing Model. *Journal of Portfolio Management*, 23:15–17, 1996.

[7] J. C. Cox, J. E. Ingersoll, and S. A. Ross. A Theory of the Term Structure of Interest Rates. *Econometrica*, 53:385–407, 1985.

[8] J. C. Cox and S. A. Ross. The Valuation of Options for Alternative Stochastic Processes. *Journal of Financial Economics*, 3:145–166, 1976.

[9] E. Derman and I. Kani. Riding on a Smile. *Risk*, 7:32–39, 1994.

[10] C. G. Ding. Algorithm AS275: Computing the Non-central Chi-square Distribution Function. *Applied Statistics*, 41:478–482, 1992.

[11] B Dupire. Pricing with a Smile. *Risk*, 7:18–20, 1994.

[12] R. Durrett. *Brownian Motion and Martingales in Analysis*. Wadsworth Advanced Books, Belmont, California, 1984.

[13] R. Durrett. *Stochastic Calculus: A Practical Introduction*. CRC Press, Boca Raton, Florida, 1996.

[14] D. C. Emanuel and J. D. MacBeth. Further Results on the Constant Elasticity of Variance Call Option Pricing Model. *Journal of Financial and Quantitative Analysis*, 17:533–554, 1982.

[15] W. Feller. Two Singular Diffusion Problems. *The Annals of Mathematics*, 54:173–182, 1951.

[16] P. Glasserman. *Monte Carlo Methods in Financial Engineering*. Springer-Verlag, New York, 2003.

[17] A. Göing-Jaeschke and M. Yor. A Survey and Some Generalizations of Bessel Processes. *Bernoulli*, 9:313–349, 2003.

[18] P. S. Hagan, D. Kumar, A. S. Lesniewski, and D. E. Woodward. Managing Smile Risk. *Wilmott*, pages 84–108, September 2002.

[19] S. L. Heston. A Closed-Form Solution for Options with Stochastic Volatility with Applications to Bond and Currency Options. *Review of Financial Studies*, 6:327–343, 1993.

[20] J. C. Hull. *Options, Futures, and Other Derivatives*. Prentice Hall, Prentice Hall, New Jersey, 6 edition, 2008.

[21] J. C. Hull and A. D. White. The Pricing of Options on Assets with Stochastic Volatilities. *Journal of Finance*, 42:281–300, 1987.

[22] I. Karatzas and S. E. Shreve. *Brownian Motion and Stochastic Calculus*. Springer-Verlag, New York, 1991.

[23] A. Lewis. *Option Valuation under Stochastic Volatility*. Finance Press, Newport Beach, 2000.

[24] H. P. McKean, Jr. *Stochastic Integrals*. Academic Press, New York, 1969.

[25] R. C. Merton. Theory of Rational Option Pricing. *Bell Journal of Economics*, 4:141–183, 1973.

[26] D. Revuz and M. Yor. *Continuous Martingales and Brownian Motion*. Springer-Verlag, New York, 3 edition, 1999.

[27] M. D. Schroder. Computing the Constant Elasticity of Variance Option Pricing Formula. *Journal of Finance*, 44:211–19, 1989.

[28] A. F. Siegel. The Non-Central Chi-squared Distribution with Zero Degrees of Freedom and Testing for Uniformity. *Biometrika*, 66:381–386, 1979.

[29] J. Takeuchi. Potential Operators Associated with Absorbing Bessel Processes. *Proceedings of the Japan Academy, Series A*, 56:93–96, 1980.